CO_2 Splitting by H_2O to CO and O_2 under UV Light in TiMCM-41 Silicate Sieve

Wenyong Lin, Hongxian Han, and Heinz Frei*

Physical Biosciences Division, Mailstop Calvin Laboratory, Lawrence Berkeley National Laboratory, University of California, Berkeley, CA 94720

Abstract

The 266 nm light-induced reaction of CO_2 and H_2O gas mixtures (including isotopic modifications $^{13}CO_2$, $C^{18}O_2$, and D_2O) in framework TiMCM-41 silicate sieve was monitored by in-situ FT-IR spectroscopy at room temperature. Carbon monoxide gas was observed as the sole product by infrared, and the growth was found to depend linearly on the photolysis laser power. H_2O was confirmed as stoichiometric electron donor. The work establishes CO as the single photon, 2-electron transfer product of CO_2 photoreduction by H_2O at framework Ti centers for the first time. O_2 was detected as co-product by mass spectrometric analysis of the photolysis gas mixture. These results are explained by single UV photon-induced splitting of CO_2 by H_2O to CO and surface OH radical.

1. Introduction

The photoreduction of CO_2 by H_2O is one of the most important chemical reactions for solar energy-to-fuel conversion. First reports on the reaction by a heterogeneous photochemical approach were by Hemminger et al. and by Inoue et al. using TiO_2, $SrTiO_3$, or SiC semiconductor powders or single crystals.[1,2] Bandgap excitation by UV light led to the formation of methane and methanol as products. Most semiconductor studies were conducted with aqueous suspensions of colloidal particles of TiO_2, ZnS, ZnSe, CdSe, etc., often surface-modified to enhance efficiency, selectivity, or wavelength response.[3,4] Reduction is initiated by transfer of photogenerated conduction band electrons to surface-adsorbed CO_2 or carbonate. Excitation wavelengths are limited to the UV region for those materials that are stable under use (metal oxides). Visible light-induced reduction of CO_2 to CO or formic acid is achieved with low bandgap semiconductor particles such as ZnSe, ZnS, or CdS, but these semiconductors require sacrificial reductants in order to suppress irreversible oxidation of the material. Likewise, visible light-activation of CO_2 in the presence of transition metal colloids requires sacrificial organic donors.[5]

Substantially improved yields of CH_3OH and CH_4 from CO_2 and H_2O under UV light were found by Anpo and co-workers over the past several years by engaging isolated tetrahedral Ti centers of micro or mesoporous silicate sieves instead of dense phase TiO_2 materials.[6,7] Molecular sieves used are microporous Ti silicalite (TS-1),[8]

zeolite Ti-beta,[9] or mesoporous framework substituted Ti silicates like TiMCM-41.[8,10] The product distribution between methanol and methane was influenced by the hydrophilic character of the solid.[9] Overall yields were found to be higher for mesoporous than microporous silicate hosts. Development of framework Ti-containing mesoporous silicate films that are optically transparent (as opposed to the light-scattering pressed wafers of crystallites) has allowed the determination of the quantum efficiency, which is around 0.3% (300 nm).[11,12] UV photolysis of CO_2 and H_2O gas mixtures loaded into the sieve was typically conducted at moderately elevated temperature (around 325 K) and monitored by GC analysis of the products. Methanol and methane were the main products, along with trace amounts of CO, O_2, C_2H_4, and C_2H_6.[6,7] Mechanistic insights were sought by EPR spectroscopy of TiO_2 samples irradiated at 77 K, resulting in the detection of H atoms and carbon radicals (elemental C and CH_3).[13,14] It was proposed that CO_2 reduction and H_2O splitting proceed competitively at the LMCT-excited Ti-O centers: CO_2 is reduced to CO, and subsequently to C radicals while H_2O photodecomposes to H and OH radicals. Reaction of H and OH radicals with carbon species is thought to yield CH_3OH and CH_4.[8,13,14]

Understanding of the mechanism of UV light-induced reduction of CO_2 by H_2O in Ti silicate sieves under reaction conditions would greatly aid in the design of photoreactors that accomplish the chemistry at longer wavelengths. Of particular interest is the identification of the individual reaction steps leading to the final products, photon-by-photon. Equally important is knowledge of the number of quanta needed to reach CH_3OH (6-electron transfer) or CH_4 (8 electrons). Moreover, possible distructive cross

reactions of intermediates or final products need to be identified since they invariably limit the quantum efficiency. In our first attempt to address these questions, we report here an in-situ FT-IR and mass spectrometric study of 266 nm-induced CO_2 reduction by H_2O in framework TiMCM-41 silicate sieve at room temperature. The work led to the identification of the single-photon 2-electron products under reaction conditions.

2. Experimental

TiMCM-41 sieve was prepared following a modified method for MCM-41 synthesis,[15] but now including a Ti precursor in the synthesis gel. Briefly, 2.2 g of CTAB template (cetyltrimethylammonium bromide, Aldrich) were dissolved in 52 mL of water at 40°C. Ammonium hydroxide (Aldrich, 26 mL) was then added under stirring. Addition of 10 mL tetraethoxysilane (Fluka, puriss.) and 0.03 g of Ti tetrabutoxide to the solution was followed by continued stirring for 3 h at RT. The gel was transferred to a Teflon-lined autoclave and held at 110°C for 48 h. Filtration and washing with distilled H_2O gave the product. Template removal was typically conducted by heating at 300°C for 2 h followed by calcination under O_2 flow at 550°C for 12 h. Template removal in some cases was also done by the ion exchange method using 0.2 M $(NH_4)_2SO_4$ in an ethanol-H_2O 1:1 solution.[16] As-synthesized Ti-MCM-41 (100 mg) was dispersed in 30 mL solution and stirred at 65^{o}C for 30 min., filtered while hot, and washed with cold ethanol. The procedure was repeated 3 times and followed by additional washing with water and ethanol to remove excess ammonium sulfate. The product was dried at 100^{o}C for 12 h

before use. Chemical analysis indicated at Ti/Si ratio of 0.020 $\pm$ 0.001. Powder XRD measurements (Siemens model D500 Cu K_α) of the sieve showed the same well-known Bragg peaks of neat MCM-41.[17] No extra peak or phase was detected. The parent MCM-41 material was prepared by the same procedure as TiMCM-41 without the Ti-source.

XANES spectra of the Ti K-edge of pressed wafers of TiMCM-41 recorded at beamline 9.3.1 at the Advanced Light Source showed a sharp, intense pre-edge peak at 4968 eV (for experimental details of the X-ray absorption measurement, see Ref. 18). The band, shown in Figure 1a, is attributed to the A_1-T_2 absorption of tetrahedrally coordinated Ti centers. Its height relative to that of the K-edge is a measure of the fraction of Ti in tetrahedral coordination.[19] Comparison with literature XANES spectra of TiMCM-41confirmed the high yield of tetrahedrally substituted Ti centers.[20] Furthermore, the UV diffuse reflectance spectra of the material (Shimadzu model UV-2100 spectrometer equipped with an integrating sphere model ISR-260) exhibit an absorption with an onset at 330 nm (Figure 1b). The short wavelength onset of the band shows that it originates from the LMCT transition of tetrahedrally coordinated Ti, in agreement with literature spectra.[21]

For photochemical experiments, 10 mg of TiMCM-41 powder was pressed into a self-supporting wafer. The wafer was mounted in a miniature infrared vacuum cell equipped with CaF_2 windows.[22] Dehydration of the sieve was accomplished by room temperature evacuation (turbomolecular pump Varian model V-70) prior to a 3-fold exchange with D_2O vapor (12 Torr). Reactants were loaded into the molecular sieve from

the gas phase through a vacuum manifold. Chemistry was monitored in situ by FT-IR spectroscopy at 0.25 cm^{-1} resolution (Bruker models IFS88 or IFS66V equipped with LN_2 cooled MCT detectors model Kolmar KMPV8-1-J2 with an 8 micron bandgap). Photolysis was conducted at RT using the 266 nm emission of a pulsed Nd:Yag laser at 10Hz (Quanta Ray model DCR2A with GCR3 upgrade). For monitoring of O_2 formation, the gas phase of the infrared cell was probed before and after photolysis by a quadrupole mass spectrometer Pfeiffer model Omnistar 422.

CO_2 (Matheson, 99.995%), $^{13}CO_2$ (ISOTEC, 99%^{13}C), $C^{18}O_2$ (ICON, 98.7%^{18}O), CO (Matheson, 99.99%), and ^{13}CO (Matheson, 99%^{13}C) were used as received. Triply distilled H_2O and D_2O (Aldrich, 99.96%D) were degassed by four freeze-pump thaw cycles before use.

3. Results

Loading of 12 Torr H_2O (D_2O) into the miniature infrared cell containing a TiMCM-41 wafer gave rise to a very broad water stretching absorption with a maximum at 3300 cm^{-1} (2500 cm^{-1}) and a bending mode at 1630 cm^{-1}. D_2O was chosen in many experiments in order to keep the 1600-1700 cm^{-1} range free of reactant absorption. Possible CO_2 reduction products such as formic acid or formate ion[23] would be difficult to detect in the presence of H_2O with its strong bending mode absorption. Subsequent addition of 700 to 750 Torr $^{12}CO_2$, $^{13}CO_2$, or $^{12}C^{18}O_2$, resulted in gas phase infrared bands

reported previously.[23] No peaks due to carbon dioxide adsorbed on the sieve were observed except for a small band at 1381 cm^{-1} ($^{13}CO_2$, 1366 cm^{-1}; $C^{18}O_2$, 1334 cm^{-1}), assigned to the ν_1 symmetric stretch of CO_2.[24] While infrared-forbidden for the gas phase molecule, the mode is induced by interaction with the nanopore environment in the case of the adsorbed CO_2.

When irradiating the loaded TiMCM-41 sieve with 266 nm light at RT, growth of gas phase CO was detected by its ro-vibrational bands in the 2200-2000 cm^{-1} region. At RT, CO generated in the silicate pores desorbs instantly into the gas phase. Figure 2 shows the infrared difference spectrum upon irradiation of a cell containing 705 Torr CO_2 and 10 Torr D_2O for 230 min. at 100 mW cm^{-2}. Aside from CO (trace b), the only additional growth was observed in the fingerprint region (trace c) at 1420 cm^{-1} and is due to HDO, presumably the result of continued slow exchange of D_2O with residual Si-OH groups of the pore surface. No other products were detected by infrared in the 4000-1300 cm^{-1} region. Specifically, no bands grew in the 2300-2200 cm^{-1} range (trace a) where C-D stretch modes of possible methanol[25] or methane[26] products would absorb. Likewise, no absorbance growth was noticed in the carbonyl stretching region (Figure 2c) where formic acid (DCO_2D, 1695 cm^{-1}),[23] formate (DCO_2^-, 1565 cm^{-1}),[23] or carbonate (CO_3^{2-}, 1440 cm^{-1}, HCO_2^-, 1600 cm^{-1})[27] are known to absorb. In a series of experiments using $^{13}CO_2$ (740 Torr) + D_2O (12 Torr) mixtures, the gas content of the infrared cell (3.4 cm^3 volume) was transferred to a quadrupole mass spectrometer for analysis before and after photolysis. Figure 3 shows the average signal observed at mass 32 in four experiments, each conducted with a new TiMCM-41 wafer. Trace (a) is the spectrum before

photolysis; the small signal at mass 32 is due to O_2 generated by $^{13}CO_2$ fragmentation in the mass spectrometer. Figure 3b shows that O_2 is produced by photolysis of $^{13}CO_2$ + H_2O at 266 nm. While well above background for each run, the signal fluctuated from experiment-to-experiment by as much as a factor of four. These fluctuations can be understood on the basis of the proposed mechanism of O_2 generation, namely dismutation of surface OH radicals, discussed in Sect. 4. We conclude that gas phase CO and O_2 are the only products formed upon 266 nm photolysis of CO_2 and H_2O in TiMCM-41 at RT.

Carbon monoxide is only produced when water is present as donor. Figure 4b shows the infrared absorbance growth of a single ro-vibrational line of CO at 2173 cm^{-1} upon irradiation of a CO_2 + H_2O mixture in TiMCM-41 for 75 min at 194 mW cm^{-2}. Trace (a) of Figure 4 is the spectrum observed when repeating the same photolysis experiment without added H_2O. We attribute the small CO growth, which occurs only during the initial 30 min. of irradiation to the presence of residual H_2O in the sieve.

Infrared monitoring of $^{13}CO_2$ + H_2O photolysis revealed the formation of some ^{12}CO gas along with the ^{13}CO product, with the ^{12}CO growth fluctuating erratically between experiments. This points to the presence of small amounts of carboneous residues that react with oxidizing intermediates formed during the photochemical reaction. Such carboneous residues are known to be difficult to remove completely from the high-surface area mesoporous silicates.[28,29] The origin of ^{12}CO was confirmed experimentally by our finding that the ^{12}CO yield decreased by a factor of 2 when conducting the experiment with a $C^{18}O_2$ + $H_2{}^{16}O$ mixture instead of the $^{13}C^{16}O_2$ + $H_2{}^{16}O$

sample. The result demonstrates that half of the O atoms of the ^{12}CO impurity produced by the photochemical reaction originate from CO_2, the other half from H_2O. Therefore, the carboneous residues in the sieve act as a trap for transient oxygen species that otherwise would react to form O_2.

In order to determine whether single or multiple photons are required for the CO production, we examined the laser power dependence of the ^{13}CO absorbance in $^{13}CO_2$ + D_2O experiments. Figure 5a shows the growth of the ro-vibrational line of ^{13}CO at 2117 cm^{-1} that was used for the analysis. As can be seen from the bands measured after consecutive photolysis periods, the FWHM is constant in the growth range used for the analysis, permitting the use of peak absorbances. Experiments were conducted by measuring the growth of the 2117 cm^{-1} peak for 16 consecutive photolysis periods of 5 min. duration, alternating between 80 and 160 mW cm^{-2} laser power. Absorbance growth data for each of the two power levels were averaged. Calibration of the 2117 cm^{-1} band intensity in terms of ^{13}CO pressure using an authentic ^{13}CO sample allowed us to determine the quantity of ^{13}CO produced in the IR cell. As can be seen from Figure 5b, the carbon monoxide growth depends linearly on the photolysis laser intensity. The slightly less than doubling of the growth at 160 mW cm^{-2} is consistent with the additional thermal heating by a few degrees caused by the increased laser power, resulting in additional desorption of reactants and products. Since saturation effects can be ruled out at the modest photolysis light intensities used, the linear dependence implies that CO is produced by a single photon process.

4. Discussion and Conclusions

The essential results of the spectroscopic study of the photolysis of carbon dioxide and water in TiMCM-41 sieve are the establishment of CO as single photon 2-electron transfer product, and O_2 as co-product under reaction conditions at RT. Water is confirmed as stoichiometric electron donor. Both CO and O_2 were already detected previously by Anpo and coworkers as trace products by GC measurements.[6,7] The importance of the work reported here is the finding that single photon excitation of the Ti-O LMCT chromophore results in splitting of CO_2 to CO with H_2O acting as donor, which has not been established before. The oxidating fragments generated by the H_2O oxidation and CO_2 dissociation react to produce O_2.

Based on these observations, the mechanism shown in Figure 6 is proposed. Excitation of the Ti-O LMCT transition of Ti centers leads to transient Ti^{+III} and a hole on a framework oxygen. Electron transfer from Ti^{+III} to CO_2 splits the molecule into CO and O^-. The latter is spontaneously protonated by a Si-OH group, or H^+ co-generated upon H_2O oxidation to yield a surface OH radical. Another such surface OH radical is formed as a result of the concurrent H_2O oxidation by the framework oxygen hole. The OH radicals either combine to yield H_2O_2 or dismutate to give O_2 and H_2O. In this UV photolysis experiment it is not possible to determine whether or not hydrogen peroxide is formed because, according to our study of H_2O_2 interacting with Ti silicate, it can react with Ti centers to yield TiOOH moieties. The latter photo-dissociates to H_2O and oxygen

at wavelengths shorter than 500 nm.[30] Figure 6 indicates the free energies associated with the formation of the stable products. The only speculative energy is that of the surface OH radicals. The free energy of the reaction $CO_2 + H_2O \rightarrow CO + 2\ OH$, with all species in the gas phase, is +139.7 kcal mol^{-1}.[31] The maximum energy available in a single photon process with 266 nm quanta is 107 kcal mol^{-1}. This implies that the OH radicals must be stabilized by interaction with the silica pore surface by at least 16 kcal mol^{-1} each, which is plausible. In light of the long lifetime of even very small radicals in a room temperature molecular sieve due to random walk (hundreds of microseconds for HCO in zeolite Y)[32], it is not surprising that, even at a very low concentration, carboneous residues offer a significant trapping mechanism for OH radicals.

It is interesting to note the difference in the 2-electron transfer product of CO_2 reduction on a Ti silicate sieve depending on whether H_2O or CH_3OH is used as donor. We have previously found that CO_2 photoreduction in Ti silicalite when using methanol as donor generates HCO_2H, not CO, as the primary reduction product.[23] This is most probably due to the fact that one-electron oxidation of CH_3OH by the hole on framework O produces CH_2OH radical, a H atom donor that can reduce transient CO_2^- to HCO_2H. By contrast, no H atom donor is generated upon H_2O oxidation that would quench CO_2^-, resulting in spontaneous splitting of the transient. In fact, the lack of accumulation of highly reactive reducing radicals constitutes an advantage of photochemical CO_2 splitting by H_2O over other photosynthetic reactions because back reaction with oxidized transient (OH radicals) does not occur. The reduced species formed by CO_2 splitting (CO) desorbs

from the reactor, leaving behind the same oxidizing species produced by photooxidation of the donor (OH).

With CO_2 splitting identified as the key activation step, redox centers can be explored that may afford the reduction of CO_2 by H_2O with photons at longer wavelengths.

Acknowledgement

This work was supported by the Director, Office of Science, Office of Basic Energy Sciences, Division of Chemical, Geological and Biosciences of the U.S. Department of Energy under contract No. DE-AC03-76SF00098.

References

[1] Hemminger, J.C.; Carr, R.; Somorjai, G.A. *Chem. Phys. Lett*. **1978**, *57*, 100.

[2] Inoue, T.; Fujishima, A.; Konishi, S.; Honda, K. *Nature* **1979**, *277*, 637.

[3] Halmann, M.M. *Chemical Fixation of Carbon Dioxide*; CRC Press; Boca Raton, 1993; p. 131.

[4] Linsebigler, A.L.; Lu, G.; Yates, Jr., J.T. *Chem. Rev*. **1995**, *95*, 735.

[5] Mandler, D.; Willner, I. *J. Am. Chem. Soc.* **1987***, 109*, 7884.

[6] Anpo, M.; Takeuchi, M. *J. Catal*. **2003,** *216*, 505.

[7] Matsuoka, M.; Anpo, M. *J. Photochem. Photobiol. C*: *Photochem*. *Rev*. **2003**, *3*, 225.

[8] Anpo, M.; Yamashita, H.; Ikeue, K.; Fujii, Y.; Zhang, S.G.; Ichihashi, Y.; Park, D.R.; Suzuki, Y.; Koyano, K.; Tatsumi, T. *Catal. Today* **1998**, *44*, 327.

[9] Ikeue, K.; Yamashita, H.; Anpo, M.; Takewaki, T. *J. Phys. Chem. B* **2001**, *105*, 8350.

[10] Zhang, S.G.; Fujii, Y.; Yamashita, H.; Koyano, K.; Tatsumi, T.; Anpo, M. *Chem. Lett*. **1997**, *659*.

[11] Ikeue, K.; Nozaki, S.; Ogawa, M.; Anpo, M. *Catal. Lett.* **2002**, *80*, 111.

[12] Shioya, Y.; Ikeue, K.; Ogawa, M.; Anpo, M. *Appl. Catal. A: General* **2003**, *254*, 251.

[13] Anpo, M.; Chiba, K. *J. Mol. Catal*. **1992**, *74*, 207.

[14] Anpo, M.; Yamashita, H.; Ichihashi, Y.; Ehara, S. *J. Electroanal. Chem*. **1995**, *396*, 21.

[15] Lin, W.; Cai, Q.; Pang, W.; Yue, Y; Zou, B. *Microporous Mesoporous Mater*. **1999***, 33*, 187.

[16] Lang, N.; Delichere, P.; Tuel, A. *Microporous Mesoporous Mater.* **2002**, *56*, 203.

[17] Beck, J.S.; Vartuli, J.C.; Roth, W.J.; Leonowics, M.E.; Kresge, C.T.; Schmitt, K.D.; Chu, C.T.W.; Olson, D.H.; Sheppard, E.W.; McCullen, S.B.; Higgins, J.B.; Schlenker, J.L. *J. Am. Chem. Soc*. **1992**, *114*, 10834.

[18] Yeom, Y.H.; Frei, H. *J. Phys. Chem. A* **2001**, *105*, 5334.

[19] Babonneau, F.; Doeuff, S.; Leaustic, A.; Sanchez, C.; Cartier, C; Vardaguer, M. *Inorg. Chem*. **1988**, *27*, 3166.

[20] Tanev, P.T.; Chilwe, M.; Pinnavaia, T.J. *Nature* **1994**, *368*, 321.

[21] Corma, A.; Navarro, M.T.; Perez, J. *J. Chem. Soc. Chem*. *Commun*. **1994**, 147.

[22] Blatter, F.; Frei, H. *J. Am. Chem. Soc.* **1994**, *116*, 1812.

[23] Ulagappan, N.; Frei, H. *J. Phys. Chem. A* **2000**, *104*, 7834.

[24] Herzberg, G. *Infrared and Raman Spectra*; Van Nostrand: New York, 1945; p. 274.

[25] Shimanouchi, T. *Tables of Molecular Vibrational Frequencies Volume I;* Natl. Bur. Stand. (U.S.), 1972.

[26] Herzberg, G. *Infrared and Raman Spectra;* Van Nostrand: New York, 1945; p. 307.

[27] Schilke, T.C.; Fisher, I.A.; Bell, A.T. *J. Catal.* **1999**, *184*, 144.

[28] Kleitz, F.; Schmidt, W.; Schuth, F. *Microporous Mesoporous Mater.* **2003**, *65*, 1.

[29] Pradhan, A.R.; Wu, J.F.; Jong, S.J.; Tsai, T.C.; Liu, S.B. *Appl. Catal. A: General* **1997**, *165*, 489.

[30] Lin, W.; Frei, H. J. *Am. Chem. Soc.* **2002**, *124*, 9292.

[31] Stull, D.R.; Prophet, H. *JANAF Thermochemical Tables Vol. 37, 2nd ed.;* Natl. Stand. Ref. Data Ser., Natl. Bur. Stand. (U.S.), 1971; p. 1.

[32] Yeom, Y.H.; Frei, H. *J. Phys. Chem. B* **2003**, *107*, 6286.

Figure Captions

Figure 1: Spectroscopic characterization of framework TiMCM-41. (a) XANES spectrum of Ti K-edge. The A_1-T_2 pre-edge peak position (4968 eV) is taken as the origin of the energy scale. (b) UV-Vis diffuse reflectance spectrum of calcined TiMCM-41 in vacuum. R = reflectance, $BaSO_4$ as the reference.

Figure 2: FT-IR difference spectrum upon 266 nm irradiation of TiMCM-41 loaded with 705 Torr CO_2 and 10 Torr D_2O for 230 min at 100 mW cm^{-2}. The negative ro-vibrational bands in (a) and (b) are due to depletion of $^{13}CO_2$ (natural abundance in $^{12}CO_2$).

Figure 3: Mass spectrum of $^{13}CO_2$ (740 Torr) + H_2O (12 Torr) mixture contained in the miniature IR cell (a) before photolysis, (b) after 266 nm irradiation for 300 min. at 160 mW cm^{-2}. The signal is the average of 4 photolysis experiments, each conducted with a fresh TiMCM-41 wafer.

Figure 4: H_2O dependence of CO_2 photoreduction. (a) CO absorbance growth at 2173 cm^{-1} upon 266 nm irradiation of TiMCM-41 loaded with 1 atm CO_2

for 75 min at 194 mW cm^{-2}. (b) Same photolysis experiment with TiMCM-41 loaded with 1 atm of CO_2 and 12 Torr H_2O.

Figure 5: Laser power dependence of $^{13}CO_2$ photoreduction by D_2O. (a) Spectra of ^{13}CO band at 2117 cm^{-1} recorded after 30 min and 80 min photolysis. (b) Laser power dependence of ^{13}CO absorbance growth. Each data point represents the average of 8 measurements.

Figure 6: Proposed mechanism for UV light-induced CO_2 reduction by H_2O at tetrahedral framework Ti centers. Energies are accurate except for surface-stabilized OH radicals (see text).

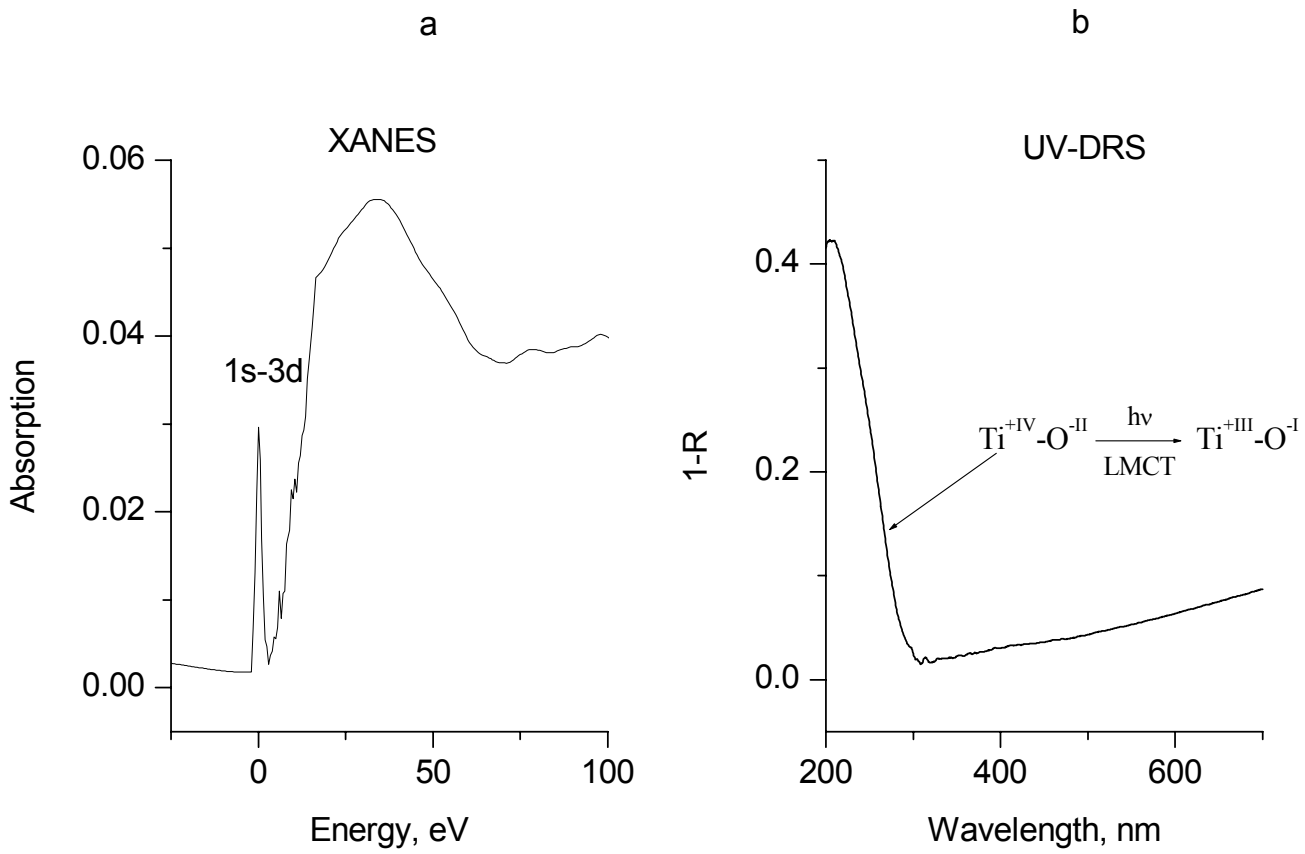
a
XANES
0.06
0.04
0.02
0.00
Absorption
1s-3d
0
50
100
Energy, eV
b
UV-DRS
0.4
0.2
0.0
1-R
Ti+IV-O-II
hν
LMCT
Ti+III-O-I
200
400
600
Wavelength, nm

Figure 1

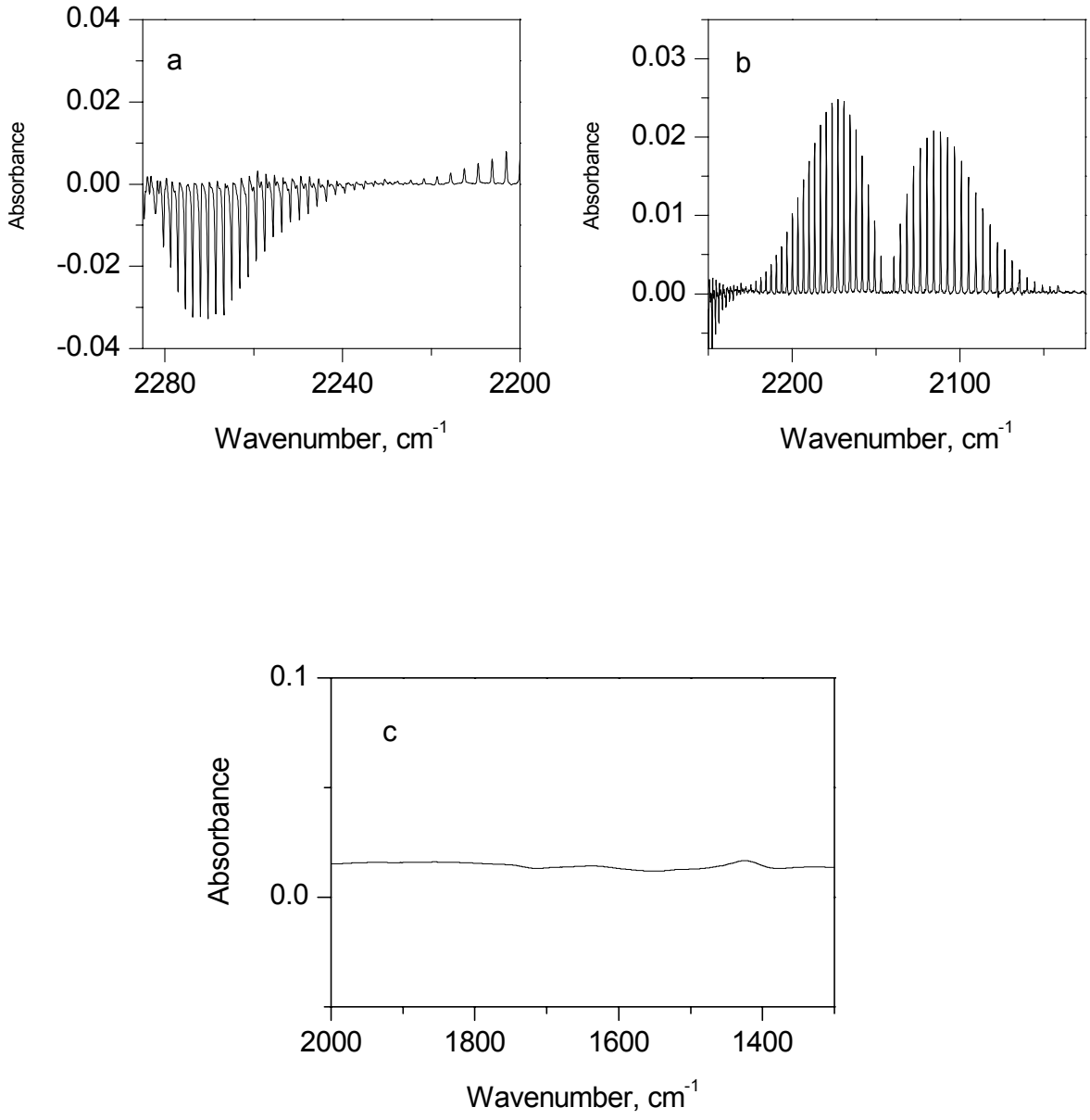
a
b
c
Absorbance
Wavenumber, cm-1
0.04
0.02
0.00
-0.02
-0.04
2280
2240
2200
0.03
0.01
2100
0.1
0.0
2000
1800
1600
1400

Figure 2

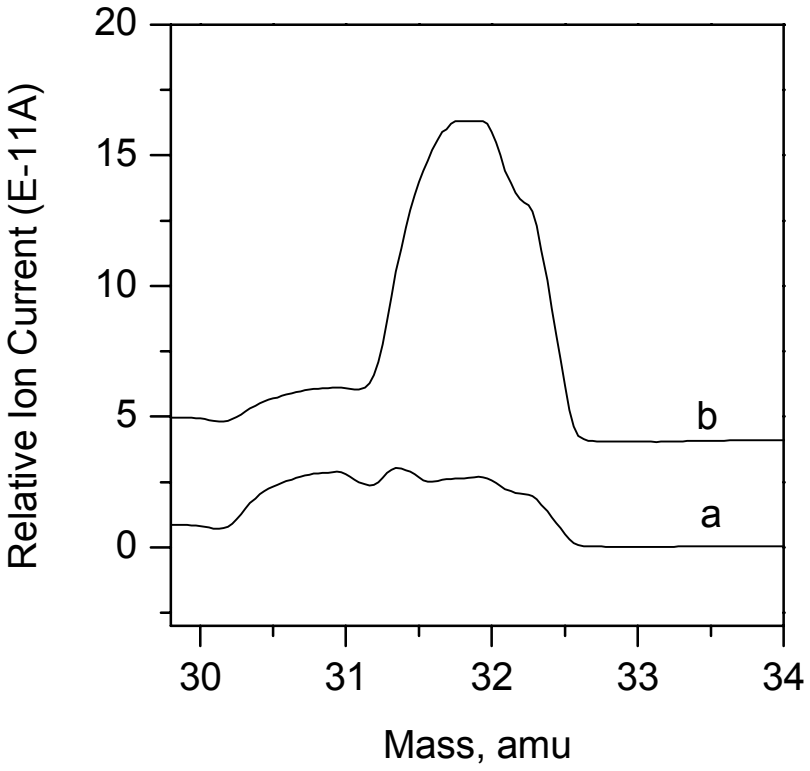

Figure 3

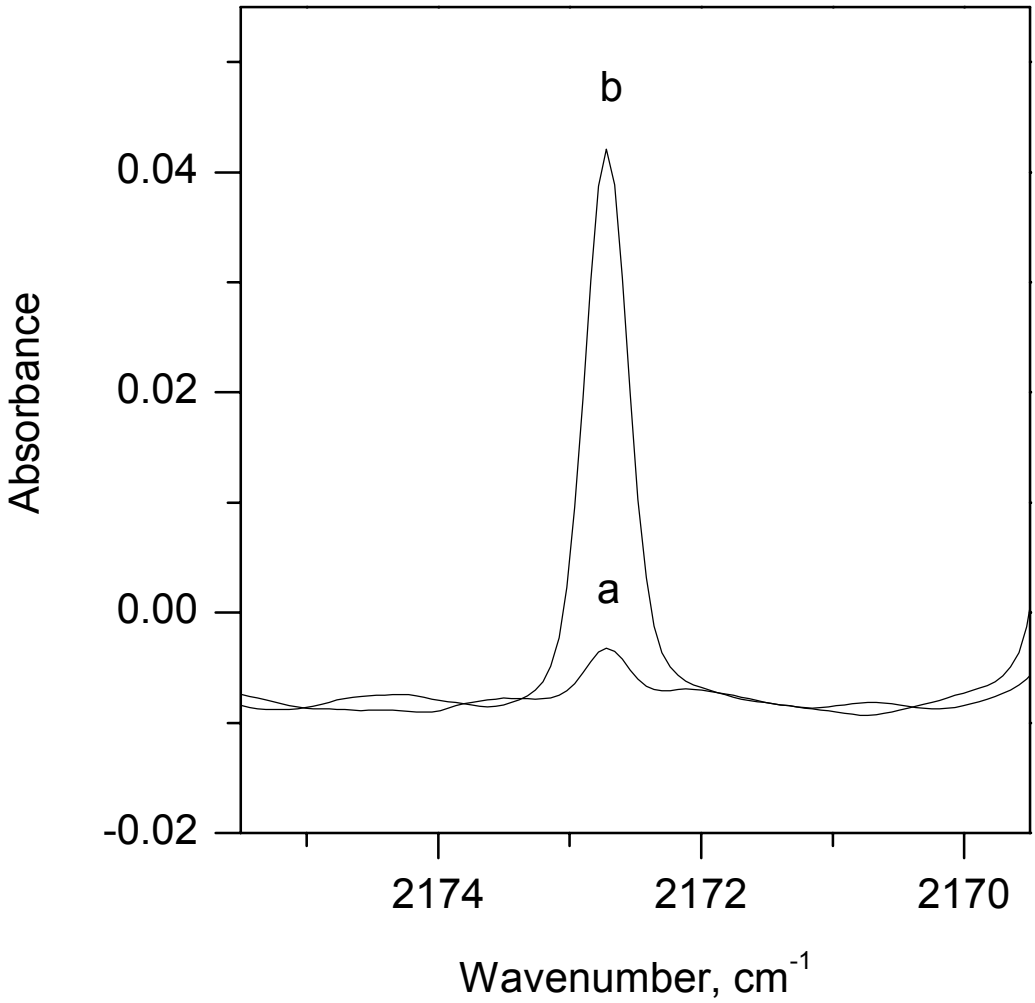

Figure 4

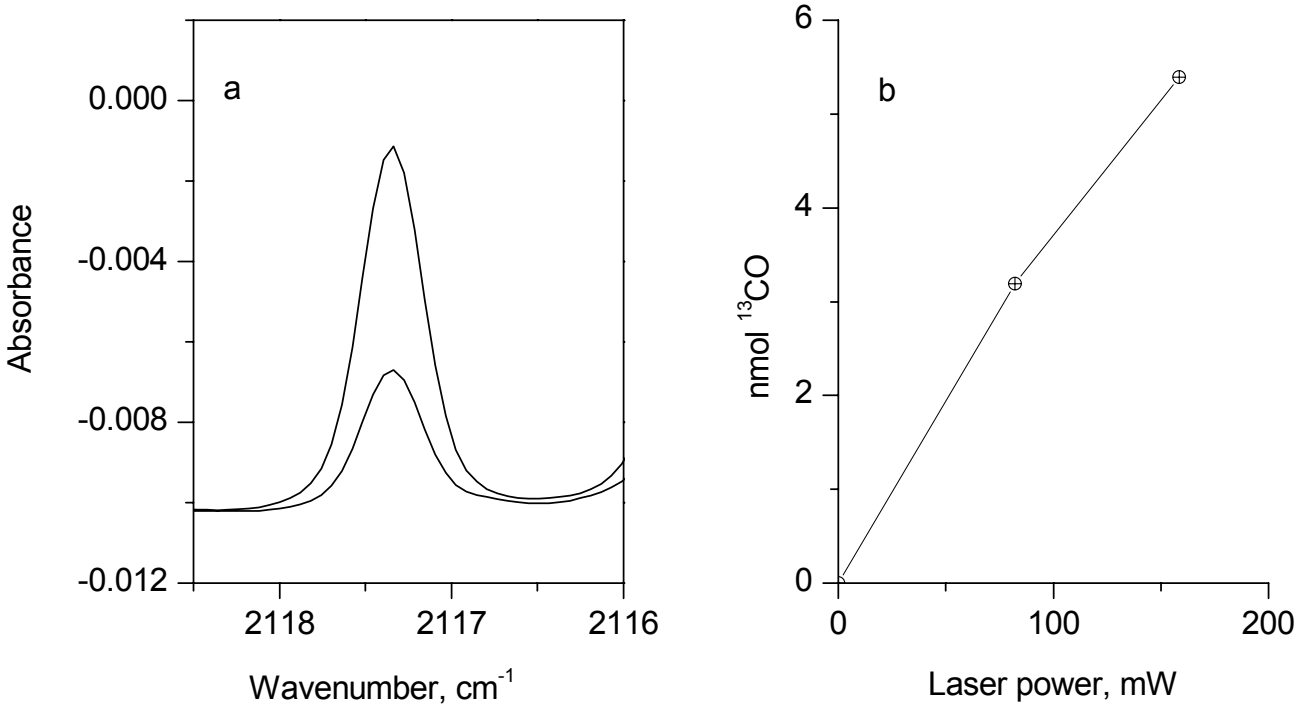
a
0.000
-0.004
-0.008
-0.012
Absorbance
2118
2117
2116
Wavenumber, cm-1
b
6
4
2
0
nmol 13CO
0
100
200
Laser power, mW

Figure 5

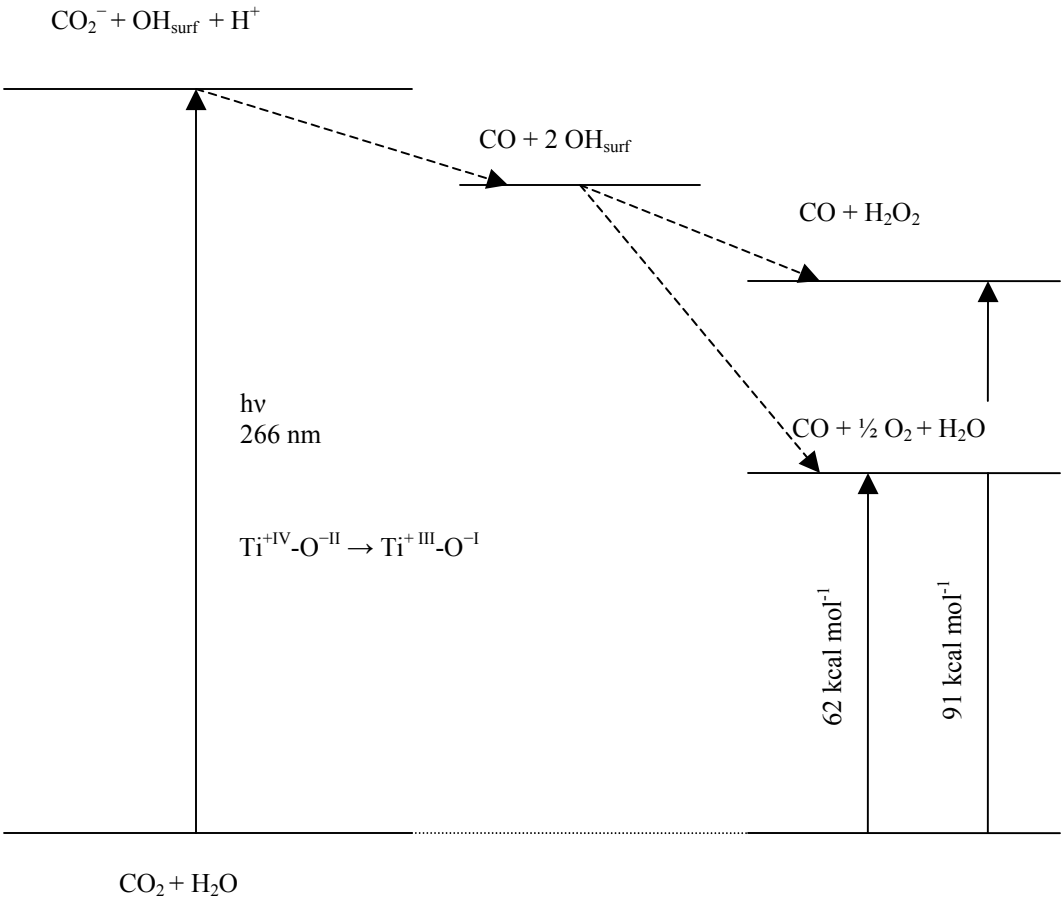
$CO_2^- + OH_{surf} + H^+$
$CO + 2\ OH_{surf}$
$CO + H_2O_2$
hν
266 nm
$CO + ½\ O_2 + H_2O$
$Ti^{+IV}\text{-}O^{-II} \rightarrow Ti^{+III}\text{-}O^{-I}$
62 kcal mol^{-1}
91 kcal mol^{-1}
$CO_2 + H_2O$

Fig 6